PHYSICAL REVIEW E **76**, 025201(R) (2007)

Global structure in spatiotemporal chaos of the Matthews-Cox equations

Hidetsugu Sakaguchi[1] and Dan Tanaka[2,*]
[1]Department of Applied Science for Electronics and Materials, Interdisciplinary Graduate School of Engineering Sciences, Kyushu University, Kasuga, Fukuoka 816-8580, Japan
[2]Department of Human and Artificial Intelligent Systems, Graduate School of Engineering, Fukui University, 3-9-1 Bunkyo, Fukui 910-8507, Japan

(Received 12 June 2007; published 13 August 2007)

We find that an amplitude death state and a spatiotemporally chaotic state coexist spontaneously in the Matthews-Cox equations and this coexistence is robust. Although the entire system is far from equilibrium, the domain wall between the two states is stabilized by a negative-feedback effect due to a conservation law. This is analogous to the phase separation in conserved systems that exhibit spinodal decompositions. We observe similar phenomena also in the Nikolaevskii equation, from which the Matthews-Cox equations were derived. A Galilean invariance of the former equation corresponds to the conservation law of the latter equations.

DOI: 10.1103/PhysRevE.76.025201 PACS number(s): 05.45.Jn, 64.75.+g, 47.52.+j

Various kinds of spatiotemporal chaos and weak turbulence are found in nonlinear nonequilibrium systems [1–4]. In most cases, spatiotemporal chaos is homogeneous in space. However, spatiotemporal chaos in some systems exhibits spatially localized structures in its fluctuations. For instance, shock waves are observed in the spatiotemporal chaos exhibited by the Kuramoto-Sivashinsky equation with stepwise boundary conditions [5], and coexistence of spatiotemporal chaos and a regular state, called a chimera state, is observed in some systems with nonlocal coupling [6–8]. In this paper, we report another mechanism of the coexistence of spatiotemporal chaos and a regular state found in the Matthews-Cox equations, which are derived from the Nikolaevskii equation. The Nikolaevskii equation is proposed as a model describing seismic waves in viscoelastic media [9,10]:

$$\frac{\partial u}{\partial t} = -\frac{\partial^2}{\partial x^2}\left[\epsilon - \left(1 + \frac{\partial^2}{\partial x^2}\right)^2\right]u - u\frac{\partial u}{\partial x}. \tag{1}$$

An equivalent equation is derived from a class of oscillatory reaction-diffusion systems [11,12]. The uniform steady state of this equation, $u=0$, is unstable with respect to finite-wavelength perturbations when the small parameter ϵ is positive. Because the equation possesses a Goldstone mode, due to its Galilean invariance, the corresponding marginally stable long-wavelength modes interact with the unstable short-wavelength modes. As a consequence, spatially periodic steady states do not appear; instead, spatiotemporal chaos is realized supercritically [13–15]. A new type of amplitude equations describing this chaos have been derived by Matthews and Cox [16]:

$$\frac{\partial A}{\partial t} = A + 4\frac{\partial^2 A}{\partial x^2} - ifA,$$

$$\frac{\partial f}{\partial t} = \frac{\partial^2 f}{\partial x^2} - \frac{\partial |A|^2}{\partial x}, \tag{2}$$

where $u \equiv \epsilon^{3/4}A(x,t)\exp(ix) + \text{c.c.} + \epsilon f(x,t) + \cdots$. The anomalous scaling $\epsilon^{3/4}$ is discussed in Refs. [16,17]. These Matthews-Cox equations also exhibit spatiotemporal chaos.

First, we numerically integrate Eq. (2) in a finite system with periodic boundaries using a split-step Fourier method. Figure 1(a) shows a time evolution of $|A|^2$. The initial conditions are $A=0$ and $f=-10\sin\{2\pi(x-L/2)/L\}$, with small perturbations, where L represents the spatial size of the system. (The cases of other initial conditions are discussed below.) As shown in this figure, $|A|^2$ is approximately equal to zero in a central small domain. In the other domains, spatiotemporal chaos appears. These results were observed previously in Ref. [18]. Figure 1(b) is an enlarged view of a chaotic region $10<x<25$ and $990<t<994$ in Fig. 1(a). The solid and dashed curves show the time evolutions of $|A(x,t)|^2$ and of $f_x \equiv \partial f/\partial x$, respectively, where a wave packet propagates from left to right. Figures 2(a) and 2(b) show $\langle |A|^2\rangle$ and $\langle f\rangle$ for $L=150$, where $\langle\cdot\rangle$ represents a long-time average. It is clearly seen that there are two spatially separated domains exhibiting the spatiotemporally chaotic state and the amplitude death state. In the former state, $\langle |A|^2\rangle \sim 5$ and $\langle f_x\rangle \sim 0.33$. In the latter state, $\langle |A|^2\rangle \sim 0$ and $\langle f_x\rangle \sim -4.65$. These values of $\langle f_x\rangle$, 0.33 and -4.65, are important in our

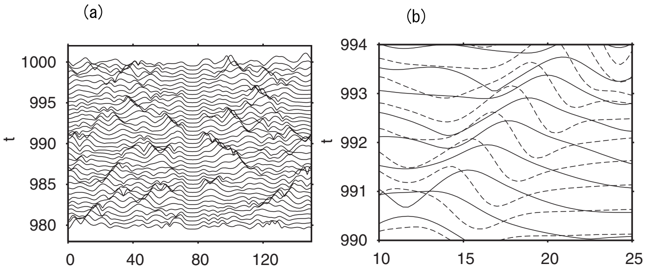

FIG. 1. (a) Temporal evolution of $|A|^2$ for $L=150$. (b) Temporal evolution of $|A|^2$ (solid curves) and f_x (dashed curves) in the region $10<x<25$ and $990<t<994$.

*dan@u-fukui.ac.jp

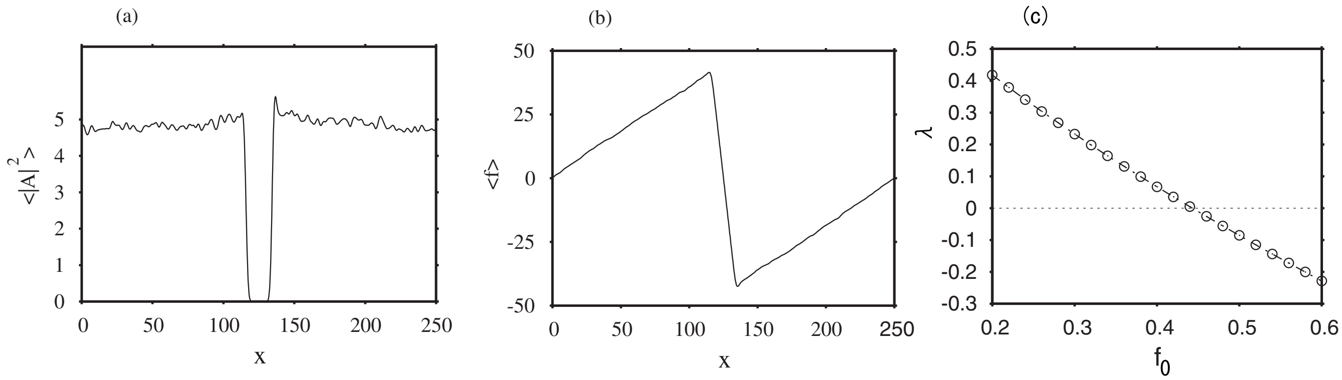

FIG. 2. (a) Temporal average of $|A|^2$. (b) Temporal average of f. (c) Maximum eigenvalue λ of the linear equation (4).

system, as discussed below, although we have not yet succeeded in determining these values theoretically. Owing to the spatiotemporal chaos, the position of the amplitude death domain fluctuates slightly. The mean position of this domain, $x \sim L/2$, is determined by the initial conditions.

In order to elucidate why these two states coexist, we consider the following linear equation with an inhomogeneous natural frequency $f(x)$ that is an approximated function of $\langle f \rangle$ around $x=L/2$ shown in Fig. 2(b):

$$\frac{\partial A}{\partial t} = A + 4\frac{\partial^2 A}{\partial x^2} - if(x)A, \tag{3}$$

where we assume that the gradient of $f(x)$ is a constant $-f_0$ in almost the entire space, except that in the neighborhood of the boundaries, the gradient is another constant required by the continuity of $f(x)$: $f(x)=-f_0\cdot(x-L/2)$ for $\Delta x/2 < x < L-\Delta x/2$, $f_0 x(L-\Delta x)/\Delta x$ for $x<\Delta x/2$ and $f_0(L-x)(L-\Delta x)/\Delta x$ for $L-\Delta x/2 < x$, where Δx is sufficiently small. Equation (3) is identical to the first equation of the Matthews-Cox equations that are linearized around $A(x,t)=0$ and $f(x,t)=f(x)$, where f is assumed to be constant in time, because temporal evolution of f is very slow in the amplitude death domain [18]. Using a Fourier expansion $A(x)=\sum_{l=-\infty}^{\infty} A_l \exp(ik_l x)$ with $k_l=2\pi l/L$, we rewrite Eq. (3) as coupled equations of A_l:

$$\frac{dA_l}{dt} = A_l - 4k_l^2 A_l + \sum_{n=1}^{\infty} \frac{2f_0}{k_n^2 \Delta x} \sin(k_n \Delta x/2)(A_{l+n} - A_{l-n}). \tag{4}$$

We numerically found that the maximum eigenvalue of the equation (4) with $\Delta x=0.1$ and $L=150$ is negative for $|f_0| > f_{0c} \sim 0.44$, as shown in Fig. 2(c). In fact, above this threshold, Eq. (3) exhibits the stable solution $A=0$. This stability is due to the inhomogeneous natural frequency $f(x)$ as studied in Ref. [19]. The amplitude death state is studied also in coupled oscillators with randomly and widely distributed natural frequencies [20]. Now, we consider the original equations (2) using the above results. Because the average value of $|f_x|$ is sufficiently larger than the critical value f_{0c} in the central small domain, as shown in Fig. 2(b), the amplitude death state is stabilized. In contrast, in the spatiotemporal chaos state, $\langle |A|^2 \rangle$ is not equal to zero, because $\langle f_x \rangle$ is smaller than the critical value and $|A|^2$ and f_x fluctuate in time. That is, $|A|^2$ increases (decreases) at a spatial point where $|f_x|$ is smaller (larger) than the critical value. Meanwhile, f decreases (increases) at a spatial point where $\partial |A|^2/\partial x$ is positive (negative), because the latter term plays the role of a sink for f, as seen in Eq. (2). These interactions between the two modes A and f cause the propagation of wave packets of $|A|^2$, as shown in Fig. 1(b), resulting in the spatiotemporal chaos.

It is noteworthy that f satisfies the conservation law

$$f_t = -\frac{\partial j}{\partial x}, \tag{5}$$

where $j \equiv -f_x + |A|^2$. Because of this conservation law and the equation $\partial\langle f \rangle/\partial t = -\partial \langle j \rangle/\partial x = 0$, the temporal average of the current j must be homogeneously constant; i.e., $\langle f_x - |A|^2 \rangle$ is constant in the entire space. Indeed, $\langle f_x - |A|^2 \rangle \sim -4.65$ in both domains. The ratio of the sizes of the two domains is equal to the inverse ratio of $\langle f_x \rangle$ in the two domains, because the spatial average of f_x is equal to zero. This type of relation is satisfied in phase separation processes in conserved systems that exhibit a spinodal decomposition in alloys [21]. In the spinodal decomposition, the coexistence of two domains (or phases) requires equality of the chemical potentials of the two phases. However, in our system, which is far from equilibrium, such a free energy or chemical potential cannot be defined.

Next, we confirm the robustness of this coexistence of the two domains by carrying out several simulations. First, we changed the spatial size of the system, L. Figures 3(a) and 3(b) show profiles of $\langle |A|^2 \rangle$ and $\langle f \rangle$ for $L=300$. $\langle |A|^2 \rangle$ remained approximately unchanged compared with the case for $L=150$. $\langle f_x \rangle$ was unchanged too, although the maximum and minimum values of $\langle f \rangle$ were 2 times larger. The absolute value of the size of the amplitude death domain was also 2 times larger. These "enlargements" can be understood from the size ratio of the two domains, as discussed below. (The coexistence is observed for $L>45$. For smaller L, the amplitude death state is unstable.) Second, we changed the initial conditions. Figure 3(c) shows $\langle |A|^2 \rangle$ for a numerical simulation started from random initial conditions around $A=0$ and $f=0$ for $L=150$. One domain of the amplitude death state

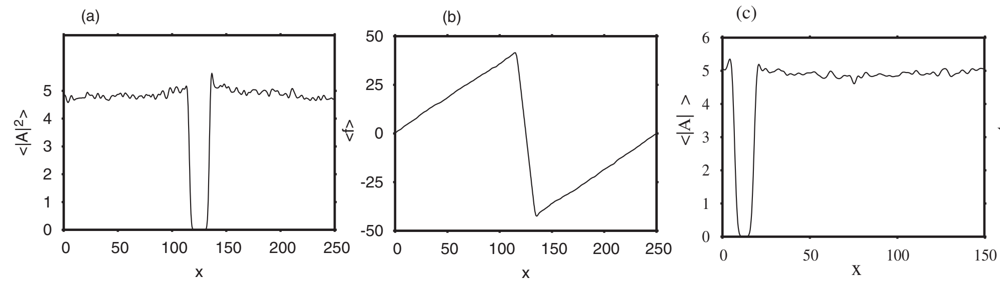

FIG. 3. (a) $\langle |A|^2\rangle$ and (b) $\langle f\rangle$ for $L=300$. (c) $\langle |A|^2\rangle$ obtained from numerical simulations with random initial conditions for $L=150$. (d) Temporal evolution of $\langle\langle |A|^2\rangle\rangle$ from the initial conditions $A=0$ and $f=-8\sin[8\pi(x-L/2)/L]$ with small perturbations for $L=150$.

appears spontaneously. (The initial condition used first in this paper is merely to locate the domain in the neighborhood of $x=L/2$.) Figure 3(d) displays the time evolution of $\langle\langle |A|^2\rangle\rangle$ for a numerical simulation started from initial conditions $A\sim 0$ and $f\sim -8\sin[8\pi(x-L/2)/L]$ for $L=150$, where $\langle\langle\cdot\rangle\rangle$ represents the average for a temporal period between $1000n$ and $1000(n+1)$ for each integer n. In a transient regime, two domains of the amplitude death state appear at $x\sim 10$ and $x\sim 75$. After this transient, the two domains merge into one. (This is analogous to the coarsening process in phase separations [21].) The above results suggest that, in the Matthews-Cox equations, the homogeneous spatiotemporally chaotic state with $\langle f_x\rangle\sim 0$ is unstable and the entire space is spontaneously and robustly separated into the two domains that exhibit the spatiotemporal chaos with $\langle f_x\rangle>0$ and the amplitude death state with $\langle f_x\rangle<0$, respectively.

To obtain an understanding of the mechanism of this robust coexistence, we consider the motion of the domain wall. The size of the amplitude death domain is relatively small in the Matthews-Cox equations (2). We find that this domain size is changed if the spatially averaged value of f_x is changed, which is presented in the following equations:

$$\frac{\partial A}{\partial t}=A+4\frac{\partial^2 A}{\partial x^2}-i\{f+f_0(x-L/2)\}A,$$

$$\frac{\partial f}{\partial t}=\frac{\partial^2 f}{\partial x^2}-\frac{\partial |A|^2}{\partial x}, \tag{6}$$

where f_0 is a nonzero constant. The two variables A and $f'\equiv f+f_0(x-L/2)$ obey the original Matthews-Cox equations, and the spatially averaged value of f'_x is f_0 ($\neq 0$), if periodic boundary conditions are assumed for A and f. Figures 4(a) and 4(b) show $\langle |A|^2\rangle$ and $\langle f'\rangle$ with $f_0=-1.4$ (solid curve) and $f_0=-2.7$ (dashed curve) for $L=150$. The initial conditions are $A=0$ and $f=0$ with small perturbations. In the domain of spatiotemporal chaos, $\langle |A|^2\rangle$ and $\langle f'_x\rangle$are approximately equal to 5 and 0.33, respectively. In the amplitude death domain, these values are approximately equal to 0 and -4.65, respectively. Although the initial conditions are $A\sim 0$ and $f\sim 0$, the amplitude death domain is located in the neighborhood of the boundaries, because the profile of f' has a jump; i.e., $|f'_x|$ is ∞ at the boundaries. The size ratio of the two domains, r, can be estimated as $r=(f_0+4.65)/4.98$, because the spatial average of f'_x is equal to $0.33r-4.65(1-r)$ $(=f_0)$. This theoretical estimation $r=(f_0+4.65)/4.98$ is confirmed numerically, as shown in Fig. 4(c), where the parameter f_0 is gradually decreased from $f_0=0$. (This fact provides an understanding of the above "enlargements.") When f_0 is equal to -4.65, the ratio r substantially vanishes. For $f_0<-4.65$, A vanishes in the entire space. For $-4.65<f_0<0.2$, the two domains characterized by the gradient values $\langle f'_x\rangle=0.33$ and -4.65 coexist, and the domain walls do not move temporally, even if f_0 is changed. This is because the conservation law of f produces a negative feedback effect on the system as follows. If the size of the chaotic domain is increased (decreased), f'_x decreases (increases) in this domain and increases (decreases) in the amplitude death domain. Thus, the stability of the amplitude death state becomes stronger (weaker). As a result, the size of the amplitude death domain tends to increase (decrease); i.e., the motion of the domain wall stops. The domain wall does not move only when $\langle f'_x\rangle$ is 0.33 and -4.65

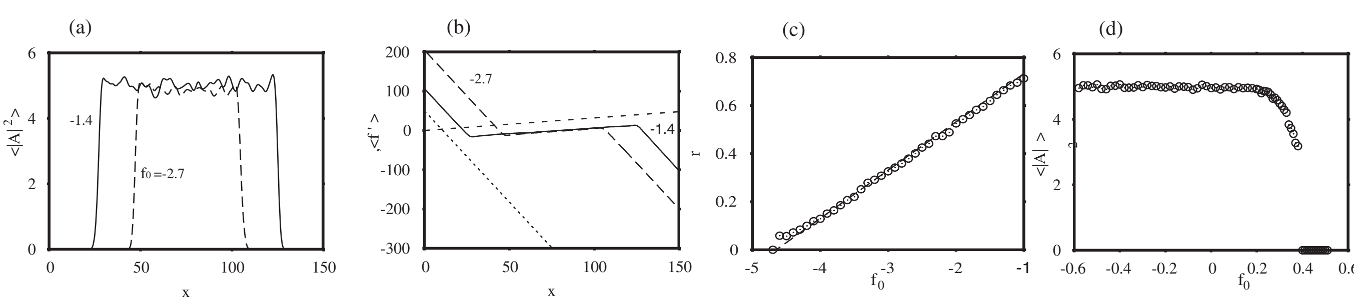

FIG. 4. (a) $\langle |A|^2\rangle$ and (b) $\langle f'\rangle$ for $f_0=-1.4$ (solid curve) and $f_0=-2.7$ (dashed curve) exhibited by Eq. (6) for $L=150$. The two lines, included for reference, have slopes of 0.33 and -4.65. (c) The size ratio of the chaotic domain, r, as a function of f_0. The dashed line is $r=(f_0+4.65)/4.98$, estimated theoretically. (d) $\langle |A|^2\rangle$ as a function of f_0.

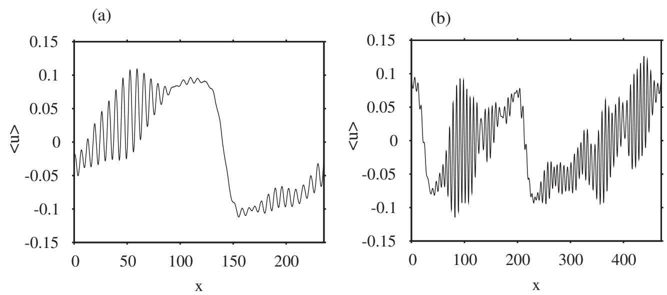

FIG. 5. (a) Temporal average of u for $L=75\pi$ and (b) for $L=150\pi$ in the Nikolaevskii equation (1) with $\epsilon=0.02$. The initial conditions are $u=-0.5\sin[2\pi(x-L/2)/L]-0.02\sin x$ with small perturbations.

in the chaotic and amplitude death domain, respectively. This is one possible origin of the coexistence of the spatiotemporal chaos and the amplitude death state.

Figure 4(d) shows $\langle|A|^2\rangle$ at $x=L/2$ as a function of f_0, where $\langle|A|^2\rangle$ is approximately equal to constant value 5 for $f_0<0.2$ and vanishes at $f_0\sim0.39$. This threshold corresponds to the following critical value. At $f_0=0.38$, $\langle f_x'\rangle\sim0.44$ in the chaotic domain. This value is close to the critical value of the linear stability of the solution $A=0$ in Eq. (3). Thus, at $f_0\gtrsim0.38$, the amplitude death state $A=0$ is stabilized in the entire space and $\langle|A|^2\rangle$ vanishes. (The temporal average $\langle f_x'\rangle$ is approximately equal to constant value 0.33 for $f_0<0.2$ in the chaotic domain.)

Finally, we show that a similar phenomenon is observed in the Nikolaevskii equation (1). Figures 5(a) and 5(b) show $\langle u\rangle$ for $L=75\pi$ and $L=150\pi$, respectively. Here $\langle\cdot\rangle$ represents an average for the time period between $t=3500$ and 4500. The global structure of $\langle u\rangle$ is reminiscent of the profile of f in the Matthews-Cox equations. In some domains (e.g., in the neighborhood of $x=20,210$ for $L=150\pi$), $\langle u\rangle$ exhibits a negative and sufficiently sharp slope. These domains correspond to the amplitude death domains exhibited by the Matthews-Cox equations, where f_x is a negative and sufficiently small value. In the other domains, $\langle u\rangle$ exhibits a positive slope as a trend. These correspond to the chaotic domains, where spatially periodic fluctuations with wave number $k\sim1$ dominate. The spatial positions of the amplitude death domains seem to move more randomly (owing to the spatiotemporal chaos) in the Nikolaevskii equation than in the Matthews-Cox equations. This difference may be due to higher harmonics, which are ignored in the Matthews-Cox equations. The domain separation becomes unclear because of the random motion of the amplitude death domain when ϵ is increased. This can be expected from the fact that, at larger ϵ, typically $\epsilon>0.1$, the two modes A and f become indistinguishable and the Matthews-Cox equations cannot describe the Nikolaevskii chaos. In fact, the Nikolaevskii equation with such large ϵ exhibits Kuramoto-Sivashinsky-like turbulence, where interaction among long wavelength modes is dominant [17].

In summary, we have found a global structure in the spatiotemporal chaos exhibited by the Matthews-Cox equations. This structure is robust and characterized by the coexistence of spatiotemporal chaos and an amplitude death state. Similar behavior was found also in the Nikolaevskii equation in the neighborhood of the onset of instability ($\epsilon\sim+0$). The amplitude death state becomes stable when the gradient of f is sufficiently large. In contrast, the spatiotemporal chaos appears when the gradient of f is not so large. That is, there exists a kind of bistability in the Matthews-Cox equations. The spatial average of f_x is fixed to be a constant, which is required by the conservation law of f. This conservation law plays the role of a negative feedback in the system, stabilizing the coexistence of the two domains. This phenomenon is analogous to the phase separation in conserved systems. Both the conservation law and bistability are essential for the domain separation, and we think that similar behavior will be observed in other systems with such bistability and conservation laws.

D.T. acknowledges a Grant-in-Aid for Young Scientists (Start Up), No. 18840020, from the Japanese Ministry of Education, Science, Sports and Culture.

[1] P. Manneville, *Disspipative Structures and Weak Turbulence* (Academic Press, Boston, 1990).
[2] T. Bohr, M. H. Jensen, G. Paladin, and A. Vulpiani, *Dynamical Systems Approach to Turbulence* (Cambridge University Press, Cambridge, England, 1998).
[3] Y. Kuramoto, *Chemical Oscillations, Waves and Turbulence* (Springer-Verlag, Berlin, 1984).
[4] I. S. Aranson and L. Kramer, Rev. Mod. Phys. **74**, 99 (2002).
[5] H. Sakaguchi, Phys. Rev. E **62**, 8817 (2000).
[6] Y. Kuramoto and D. Battogtokh, Nonlinear Phenom. Complex Syst. (Dordrecht, Neth.) **5**, 380 (2002).
[7] D. M. Abrams and S. H. Strogatz, Phys. Rev. Lett. **93**, 174102 (2004).
[8] H. Sakaguchi, Phys. Rev. E **73**, 031907 (2006).
[9] V. N. Nikolaevskiy, *Recent Advances in Engineering Science, Lecture Notes in Engineering*, Vol. 39, edited by S. L. Koh and C. G. Speciale (Springer, Berlin, 1989), p. 210.
[10] I. A. Beresov and V. N. Nikolaevskiy, Physica D **66**, 1 (1993).
[11] D. Tanaka, Phys. Rev. E **70**, 015202(R) (2004).
[12] D. Tanaka, Prog. Theor. Phys. Suppl. **161**, 119 (2006).
[13] M. I. Tribelsky and K. Tsuboi, Phys. Rev. Lett. **76**, 1631 (1996).
[14] M. I. Tribelsky and M. G. Velarde, Phys. Rev. E **54**, 4973 (1996).
[15] M. I. Tribelsky, Phys. Usp. **40**, 159 (1997).
[16] P. C. Matthews and S. M. Cox, Phys. Rev. E **62**, R1473 (2000).
[17] D. Tanaka, Phys. Rev. E **71**, 025203(R) (2005).
[18] D. Tanaka, H. Azuma, and H. Kasahara (unpublished).
[19] H. Sakaguchi, Prog. Theor. Phys. **80**, 743 (1988).
[20] R. E. Mirollo and S. H. Strogatz, J. Stat. Phys. **60**, 245 (1990).
[21] A. Onuki, *Phase Transition Dynamics* (Cambridge University Press, Cambridge, England, 2002).